Electromagnetic Vortex Fields, Spin, and Spin-Orbit Interactions in Electron Vortices

S. M. Lloyd, M. Babiker, J. Yuan, and C. Kerr-Edwards
Department of Physics, University of York, Heslington, York YO10 5DD, United Kingdom
(Received 27 July 2012; published 20 December 2012)

Electron vortices are shown to possess electric and magnetic fields by virtue of their quantized orbital angular momentum and their charge and current density sources. The spatial distributions of these fields are determined for a Bessel electron vortex. It is shown how these fields lead naturally to interactions involving coupling to the spin magnetic moment and spin-orbit interactions which are absent for ordinary electron beams. The orders of magnitude of the effects are estimated here for ångström scale electron vortices generated within a typical electron microscope.

DOI: 10.1103/PhysRevLett.109.254801 PACS numbers: 41.85.−p, 42.50.Tx

The last few years have seen the advent of electron vortices (EVs) as Schrödinger quantum states representing twisted de Broglie–type waves that can be created inside an electron microscope. They were first suggested on a theoretical basis by Bliokh *et al.* [1] and experimental reports by several groups [2–5] have established EVs as quantum states with well defined properties. They bear some resemblance to optical vortices (OVs), specifically in that they too carry orbital angular momentum (OAM) $l\hbar$ associated with the azimuthal phase factor $\exp(il\phi)$ in their wave function, where l is the winding number [6–9]. However, in addition to the OAM properties, EVs carry electron spin-$\frac{1}{2}$ angular momentum and are endowed with electric charge e. Recent studies have confirmed that the two types of vortices differ considerably in their interactions with matter, most notably in spectroscopy.

The first experimental work using EVs in electron energy loss spectroscopy (EELS) was carried out recently by Verbeeck *et al.* [3] who reported a clear dichroic signal emerging from the interaction of EVs of opposite winding numbers $l = \pm 1$ with magnetized iron film samples. The physics of the Verbeeck *et al.* experiment has subsequently been explored by Lloyd *et al.* [10] who showed that EVs are capable of exchanging OAM with the internal dynamics of an atom undergoing electric dipole transitions. Lloyd *et al.*, however, came to the conclusion that EV beams with opposite winding numbers $l = \pm 1$ should have identical EELS strengths for a nonmagnetic film and so the observed dichroism effect must be due to differences in the populations of the magnetic levels participating in the transitions. Nevertheless, the primary finding of Lloyd *et al.*'s work, namely, that EVs do engage with the internal dynamics of matter in processes involving electric dipole transitions is significant and is in sharp contrast with the case of optical vortices which have been shown not to engage with the internal dynamics in electric dipole transitions [11,12].

Research to uncover the fundamental physics of EVs has only just begun. Recent work by Bliokh *et al.* [13] considered relativistic electron vortices and analysed the role of spin and OAM and their coupling in that context. The aim of this Letter is to point out some fundamental properties of EVs associated with their orbital motion. The fact they carry electric charge e, along with their wave function ψ, implies that they are endowed with electric and magnetic fields associated with their charge and current distributions. We explore how the vortex fields would couple to the spin magnetic moment and show that they are also responsible for an interaction between the spin and the OAM of the vortex, so giving rise to a spin-orbit effect in this context.

It is well known that spin-orbit interactions play a significant role in atomic, molecular, and solid state physics. Albeit a relativistic correction, the spin-orbit coupling is strong in these contexts due to the strong Coulomb fields responsible for the bonding. Recent developments have confirmed that it is now possible to generate atomic scale EVs, so-called ångström EVs [14] since they are localized in an ångström size region.

The electron vortex is characterized by a wave function $\psi(\mathbf{r}, t)$. Since we are concerned with EVs generated inside an electron microscope, where the typical energy is of the order 200 keV, the EV is a solution of the scalar Helmholtz equation emerging from the Schrödinger equation in cylindrical polar coordinates, namely,

$$\nabla^2 \psi(\mathbf{r}, t) + \frac{2m_0 \mathcal{W}'}{\hbar^2} \psi(\mathbf{r}, t) = 0, \tag{1}$$

where $\mathcal{W}'$ is the energy eigenvalue and m_0 is the electron rest mass. We concentrate on the Bessel-type solution of this equation and write for the vortex wave function in cylindrical polar coordinates $\mathbf{r} = (\rho, \phi, z)$:

$$\psi(\mathbf{r}, t) = N_l J_l(k_\perp \rho) e^{ik_z z} e^{il\phi} e^{-i\omega t}, \tag{2}$$

where the radial function $J_l(k_\perp \rho)$ is the Bessel function of order l where l is the winding number. The wave numbers $k_\perp$ and k_z stand for in-plane and axial wave vector variables respectively, and $\omega = \mathcal{W}'/\hbar$. As pointed out earlier, the vorticity resides in the phase factor $e^{il\phi}$ and N_l is the normalization constant which follows straightforwardly in the form

$$N_l = (2\pi D \mathcal{I}_l)^{-1/2}, \tag{3}$$

where the beam length D arises in the z integration for a beam extending between $-D/2$ and $D/2$ and $\mathcal{I}_l$ is defined as

$$\mathcal{I}_l = \int_0^{\rho_{l,1}} J_l^2(k_\perp \rho)\rho d\rho. \tag{4}$$

Strictly speaking, the upper limit of the integration in Eq. (4) should be infinity. Implied in Eq. (4) is the assumption that the production of a Bessel vortex of winding number l is realized using a holographic mask of finite width, in which case we shall assume that the effective region of the vortex cross section only spans the first zero $\alpha_{l,1}$ of the Bessel function so that we can write

$$\rho_{l,1} = \frac{\alpha_{l,1}}{k_\perp} \tag{5}$$

as the radius of our Bessel vortex. This enables a connection of the theory with the measurable experimental parameters, notably the axial electric current I_z of the electron vortex. In a conventional electron microscope the beam energy is of the order of 200 keV and the operating electric current is of the order of 1 nA. Note that the fields are due to the charge and current arising from the flow of electrons associated with the vortex and we assume that electron-electron interactions are negligible, thus ignoring the Boersch effect [15]. A charge density distribution $\tilde{\rho}(\mathbf{r}, t)$ and current density distribution $\tilde{\mathbf{J}}(\mathbf{r}, t)$ are associated with the vortex wave function specified from Eq. (2) to Eq. (5). Applications of standard quantum mechanical methods [16] give

$$\tilde{\rho}(\mathbf{r}, t) = e|N_l|^2 J_l^2(k_\perp \rho), \tag{6}$$

$$\tilde{\mathbf{J}}(\mathbf{r}, t) = |N_l|^2 \frac{e\hbar}{m_0}\left(\frac{l}{\rho}\hat{\boldsymbol{\phi}} + k_z \hat{z}\right) J_l^2(k_\perp \rho). \tag{7}$$

The axial electric current I_z is the flux of the axial component of the current density through a cross section of radius $\rho_{l,1}$. Using Eq. (3) we obtain

$$I_z = 2\pi e N_l^2 \mathcal{I}_l \left(\frac{\hbar k_z}{m_0}\right) = \frac{e\hbar k_z}{m_0 D}. \tag{8}$$

The vortex charge and current distributions specified above generate electric and magnetic fields which now follow straightforwardly. Using Gauss's theorem to evaluate the electric field, it is clear that the cylindrical symmetry of the Bessel mode function leads to an electric field that has only a plane radial component and is a function of ρ only:

$$\mathbf{E}_{\mathrm{EV}}(\rho) = -\hat{\boldsymbol{\rho}} \frac{e|N_l|^2}{2\epsilon_0} \rho [J_l^2(k_\perp \rho) - J_{l-1}(k_\perp \rho) J_{l+1}(k_\perp \rho)]. \tag{9}$$

What remains is to eliminate the factor $|N_l|^2$ in favor of the measurable electric current I_z using Eq. (8). This is achieved for the Bessel beam with radius given by Eq. (5) for $l = 1$, and typical electron beam parameters. The result for the variation of $\mathbf{E}_{\mathrm{EV}}$ with ρ is shown in Fig. 1.

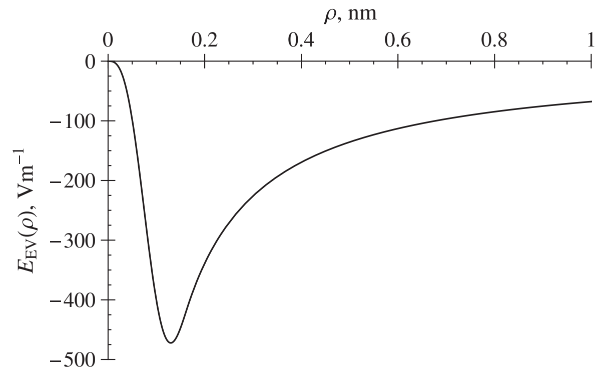

FIG. 1. The electric field of the finite vortex beam as a function of ρ, in the radial direction. The parameters used are $I_z = 1$ nA, $k_z = 2.3 \times 10^{12}$ m^{-1}, $k_\perp = 0.01 k_z$, and a beam radius, as defined in Eq. (5), equal to 0.17 nm.

The magnetic field due to the current density can also be evaluated using standard electromagnetism. We find after some algebra that there are only two components and these are functions only of the planar radial position ρ

$$\mathbf{B}_{\mathrm{EV}}(\rho) = B_\phi \hat{\boldsymbol{\phi}} + B_z \hat{\mathbf{z}}, \tag{10}$$

where B_ϕ and B_z are given by

$$B_\phi = \left(\frac{e\mu_0 |N_l|^2 \hbar k_z \rho}{2m_0}\right)[J_l^2(k_\perp \rho) - J_{l-1}(k_\perp \rho) J_{l+1}(k_\perp \rho)], \tag{11}$$

$$B_z = \left(\frac{e\mu_0 |N_l|^2 \hbar}{m_0}\right) \frac{l}{\rho} \int_\rho^\infty J_l^2(k_\perp \rho') d\rho'. \tag{12}$$

There are no closed forms of the integral in Eq. (12) and the result is obtained numerically. The variation of the two components of $\mathbf{B}_{\mathrm{EV}}$ for the Bessel beam are shown in Fig. 2.

To determine how electric and magnetic fields interact with the electron vortex, we start from the Dirac equation in the presence of electromagnetic fields, with vector and scalar potentials $\mathbf{A}$ and Φ. These potentials can be external, or they could be those corresponding to the vortex fields derived above. The appropriate Dirac equation is

$$\{(\mathcal{W} - e\Phi) - c\boldsymbol{\alpha} \cdot (\mathbf{p} - e\mathbf{A}) - \beta m_0 c^2\}\Psi(\mathbf{r}, t) = 0, \tag{13}$$

where Ψ is a four-component Dirac spinor, $\boldsymbol{\alpha}$ and β are the Dirac 4×4 matrices and $\mathcal{W}$ is the total energy, including the rest-mass energy $m_0 c^2$. Since we are primarily concerned with EVs created inside electron microscopes for which the typical energy is 200 keV, we must be satisfied with the wave function ψ given in Eq. (2), which is a

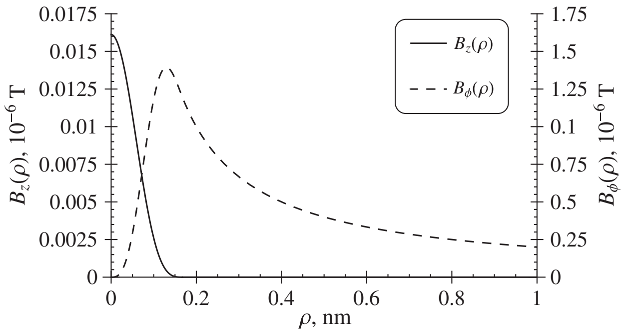

FIG. 2. The magnetic field of the vortex beam as a function of ρ, having two components, one azimuthal, $B_\phi(\rho)$ and one axial, $B_z(\rho)$. Note that $B_z(\rho)$ is 2 orders of magnitude smaller than $B_\phi(\rho)$. See the caption to Fig. 1 for parameters used.

solution of the free Schrödinger equation with the Hamiltonian $\hat{H}_0 = p^2/2m_0$. The procedure is to follow a standard path leading to the nonrelativistic limit of the Dirac equation, Eq. (13) [17]. In the nonrelativistic limit the rest energy m_0c^2 is the largest energy so we can write

$$\mathcal{W} = m_0c^2 + \mathcal{W}'; \qquad \mathcal{W}' \ll m_0c^2, \tag{14}$$

so that in the absence of any interactions $\mathcal{W}'$ would be the energy appearing in the Bessel vortex wave function of Eqs. (1) and (2). We write the Dirac spinor in terms of large and small components Ψ_a and Ψ_b, respectively, and substitute in Eq. (13). Using the Dirac representation we can eliminate the small components Ψ_b and write the equation entirely in terms of the large components Ψ_a. We find after some algebra

$$\left\{\frac{\boldsymbol{\sigma}\cdot\boldsymbol{\Pi}}{2m_0}\left(1+\frac{\mathcal{W}'-e\Phi}{2m_0c^2}\right)^{-1}\boldsymbol{\sigma}\cdot\boldsymbol{\Pi}+e\Phi\right\}\Psi_a = \mathcal{W}'\Psi_a, \tag{15}$$

where $\boldsymbol{\Pi} = \mathbf{p} - e\mathbf{A}$. So far we have not made any approximations. In the nonrelativistic regime where $\mathcal{W}' \ll m_0c^2$ and $e\Phi \ll m_0c^2$ we have

$$\left(1+\frac{\mathcal{W}'-e\Phi}{2m_0c^2}\right)^{-1} \approx 1 - \frac{(\mathcal{W}'-e\Phi)}{2m_0c^2}. \tag{16}$$

We substitute this into Eq. (15) and make use of the standard properties of the Pauli matrices, namely, that $\sigma_i\sigma_j = \delta_{ij} + i\epsilon_{ijk}\sigma_k$, where ϵ_{ijk} is the Levi-Cevita symbol. Dropping small terms consistent with the nonrelativistic regime, the procedure culminates in the Pauli equation, which we write here in a form abbreviated for our purposes as

$$(\hat{H}_0 + \hat{H}_{\rm int} + \mu\boldsymbol{\sigma}\cdot\mathbf{B} - \xi\mathbf{S}\cdot\mathbf{L})\Psi_a = \mathcal{W}'\Psi_a, \tag{17}$$

where the two-component state $\Psi_a = \psi(\mathbf{r})\chi$ is the product of a single-component space wave function $\psi(\mathbf{r})$ and a spin wave function χ where χ is one of the standard two-component spin vectors $(1,0)^T$ or $(0,1)^T$, and where $\hat{H}_0 = p^2/2m_0$ is the zero order Hamiltonian and the spin and orbital angular momentum operators $\mathbf{S}$ and $\mathbf{L}$ are the usual $\mathbf{L} = \mathbf{r}\times\mathbf{p}$ and $\mathbf{S} = \frac{1}{2}\hbar\boldsymbol{\sigma}$.

In the perturbation procedure the zero order Hamiltonian, $\hat{H}_0 = p^2/2m_0$ is the only term to be retained, which leads to the Helmholtz equation, Eq. (1). The interaction term $\hat{H}_{\rm int}$ in Eq. (17) couples the fields to the vortex momentum and charge. We have written the last two terms on the left-hand side of Eq. (17) explicitly in order to highlight the coupling of the spin to the magnetic moment of the electron and the spin-orbit coupling. The term containing $\mu = (e\hbar/2m_0)$ couples the spin magnetic moment to the magnetic fields. Finally, the last term on the left-hand side of Eq. (17) is the spin-orbit coupling with ξ the position dependent coupling factor. Note that, in general, the spin-orbit coupling term $\xi\mathbf{S}\cdot\mathbf{L}$ can only arise for central scalar potentials, i.e., those having a term of the form

$$\Phi(\mathbf{r}) = V(r); \qquad \nabla\Phi = \frac{\hat{\mathbf{r}}}{r}\frac{dV}{dr}, \tag{18}$$

where $r = |\mathbf{r}|$, in which case ξ entering the spin-orbit interaction term is given by

$$\xi = -\frac{e}{2m_0^2c^2r}\frac{dV}{dr}. \tag{19}$$

We shall now consider two cases in which the spin-orbit coupling in the electron vortex would be manifest. The first case is the scenario in which external fields are absent and the second case is the scenario in which external fields are present.

In the absence of external fields only the vortex fields operate, in which case Eq. (17) becomes

$$(\hat{H}_0 + \hat{H}_{\rm int} + \mu\boldsymbol{\sigma}\cdot\mathbf{B}_{\rm EV} - \xi(\rho)S_zL_z)\Psi_a = \mathcal{W}'\Psi_a \tag{20}$$

since $\mathbf{E} = -\boldsymbol{\nabla}\Phi$, and since the dependence of the electric field is only on ρ (i.e., the field is axially central) we have that

$$\boldsymbol{\nabla}\Phi = -\hat{\boldsymbol{\rho}}E_{\rm EV}(\rho), \tag{21}$$

with $E_{\rm EV}$ describing the magnitude of the field, such that $\mathbf{E}_{\rm EV} = E_{\rm EV}\hat{\boldsymbol{\rho}}$, and $\boldsymbol{\rho}\times\mathbf{p} = L_z\hat{\mathbf{z}}$. In this case, the spin-orbit coupling factor $\xi(\rho)$ is given by

$$\xi(\rho) = \frac{e}{2m_0^2c^2\rho}E_{\rm EV}(\rho). \tag{22}$$

As in conventional spin-orbit interaction, the electron vortex spin-orbit interaction is evaluated as a perturbation once the vortex zero-order eigenvalue problem with zero-order Hamiltonian $\hat{H}_0$ is solved, leading to the vortex energy eigenfunction, Eq. (2), and energy eigenvalue $\mathcal{W}'$. First order perturbation theory gives

$$\Delta_{(l;s_z)} = -\hbar^2 l s_z\langle\psi|\xi_l(\rho)|\psi\rangle, \tag{23}$$

where $s_z = \pm\frac{1}{2}$ and l is the vortex winding number, such that $l\hbar$ is the OAM about the z axis. For illustration we consider the simplest and most discussed electron vortex to date, namely, that for which $l = 1$. Since s_z takes the values $\pm\frac{1}{2}$ there are two quantum states. Thus, the $l = 1$ EV beam is in reality split into two beams with slightly different energies. The spin-orbit energy splitting between the states $|s_z, l\rangle = |\frac{1}{2}, 1\rangle$ and $|s_z, l\rangle = |-\frac{1}{2}, 1\rangle$ is given by

$$\delta^{\rm beam}_{1;(1/2,-1/2)} = \hbar^2\langle\psi|\xi_l(\rho)|\psi\rangle. \quad (24)$$

An evaluation of the expectation value of $\xi(\rho)$ leads to

$$\delta^{\rm beam}_{1;(1/2,-1/2)} = \frac{\hbar^2}{2}\frac{D\pi e N_1^2}{m_0^2c^2}\int_0^{\rho_{1,1}} J_1^2(k_\perp\rho)E_{\rm EV}(\rho)d\rho, \\ = \frac{\hbar^2 e}{4m_0^2c^2 I_1}\int_0^{\rho_{1,1}} J_1^2(k_\perp\rho)E_{\rm EV}(\rho)d\rho. \quad (25)$$

The order of magnitude of the spin-orbit splitting can be estimated for typical parameters in the context of electron vortices created inside electron microscopes. From Fig. 1 we can see that the electric field is of the order of a few hundred V m^{-1}; with the parameters given in Fig. 1 this gives

$$\delta^{\rm beam}_{1;(1/2,-1/2)} \approx 3\times 10^{-13}\ {\rm eV}. \quad (26)$$

As we point out below in conclusion, this is clearly too small for direct energy measurement, although we suggest that indirect measurements are, in principle, possible. In view of the parameters we have assumed, the electric and magnetic fields in electron microscope-produced EV beams generate a small spin-orbit interaction and splitting. The coupling of the magnetic field to the electron spin magnetic moment mediated by the interaction term $\boldsymbol{\sigma}\cdot\mathbf{B}_{\rm EV}$ also turns out to be small and we do not pursue its evaluation in this context.

Finally, we consider the scenario in which external fields are present, in which case the general equation, Eq. (17), applies. Having estimated here the contributions from vortex fields, we now concentrate on the spin-orbit interaction due to an external electric field. This, we assume, is provided by an ion of effective charge Ze situated on the axis of the beam at $z = 0$. The ion is assumed to be embedded in the material, as is normally assumed in conventional scattering problems [18]. The spin orbit interaction Hamiltonian is given by $-\xi(r)\mathbf{S}\cdot\mathbf{L}$. However, in the electron vortex beam case the OAM is realized only along the z axis; i.e., we must have $\mathbf{L} = L_z\hat{\mathbf{z}}$ in which case the spin-orbit interaction is $\xi(r)S_zL_z$. Since $L_z\hat{\mathbf{z}} = \boldsymbol{\rho}\times\mathbf{p}$, the spin-orbit coupling parameter is now given by

$$\xi(r) = \frac{Ze_0^2}{2m_0^2c^2(\rho^2+z^2)^{3/2}}, \quad (27)$$

where $e_0^2 = e^2/(4\pi\epsilon_0)$. Once again we consider the $l = 1$ vortex and write

$$\Delta = \langle\Psi_a|\xi(r)S_zL_z|\Psi_a\rangle. \quad (28)$$

We find the splitting between the states $|s_z, l\rangle = |\frac{1}{2}, 1\rangle$ and $|s_z, l\rangle = |-\frac{1}{2}, 1\rangle$ to be

$$\delta^{\rm external}_{1;(1/2,-1/2)} = \frac{\hbar^2 Ze_0^2}{2m_0^2c^2 D I_1}\int_0^{\rho_{1,1}}\int_{-\frac{D}{2}}^{\frac{D}{2}} \frac{J_1^2(k_\perp\rho)\rho}{(\rho^2+z^2)^{3/2}}dzd\rho. \quad (29)$$

Using the same parameters as before for an ångström beam and for orientation as regards to orders of magnitude finding spin-orbit splitting in this case to be

$$\delta^{\rm external}_{1;(1/2,-1/2)} \approx 5Z\times 10^{-13}\ {\rm eV}. \quad (30)$$

Besides Z as a scaling factor, this is comparable in magnitude to the spin-orbit splitting in Eq. (26). The expression in Eq. (29) can be shown to scale quadratically with $k_\perp$, so that the energy splitting is increased for higher values of $k_\perp$. This leads to a beam with smaller radial extent, as $\rho_{l;1}$ decreases. Hence, the largest value would be expected in the case of ångström size EVs having high transverse momenta, the generation of which is discussed in Ref. [14].

In conclusion, we have shown that besides the quantized OAM property an electron vortex possesses electric and magnetic fields which are responsible for a coupling to the spin magnetic moment, and for a spin-orbit interaction. The electric and magnetic fields arise here due to the charge and current distributions associated with the vortex. An ordinary electron beam also has both electric and magnetic fields but these differ materially from the vortex fields which are characterized by the property of orbital angular momentum. We have demonstrated that it is the fact that the vortex electric field is a function of ρ, i.e., it is a *central vector field* and that the beam carries orbital angular momentum which ensures the existence of the spin-orbit interactions due to vortex fields. The electric field of an ion situated on the beam axis is also a central field, i.e., a function of the radial coordinate r and so leads to spin-orbit coupling in the presence of the vortex. The spin-orbit energy shift is negligibly small for the EVs created within the current generation of electron microscopes for which the limit of detection in energy is about 10 meV. We envisage that indirect measurement techniques of the spin-orbit effect are possible. These would involve the scenario of creating a spin-polarized vortex beam subject to radio frequency fields and determining the variations of effects due to spin flip processes with radio frequency. This may well be achieved, especially in the next generation of electron microscopes with high brightness, high resolution, and ultra high energy. Other possibilities could involve electron vortex beams not produced inside electron microscopes but, for example, those generated in linear accelerators.

The electric and magnetic fields described here are fundamental properties of electron vortices which are of interest in their own right. They are, significantly, endowed with the property of orbital angular momentum. Work in hand indicates that these fields are important for the manipulation, i.e., translation and rotation, of small particles of matter by the electron vortex, but we shall not pursue this issue any further here.

[1] K. Y. Bliokh, Y. P. Bliokh, S. Savelev, and F. Nori, Phys. Rev. Lett. **99**, 190404 (2007).

[2] M. Uchida and A. Tonomura, Nature (London) **464**, 737 (2010).

[3] J. Verbeeck, H. Tian, and P. Schattschneider, Nature (London) **467**, 301 (2010).

[4] B. J. McMorran, A. Agrawal, I. M. Anderson, A. A. Herzing, H. J. Lezec, J. J. McClelland, and J. Unguris, Science **331**, 192 (2011).

[5] T. Gnanavel, J. Yuan, and M. Babiker, in *Proceedings of European Microscopy Congress, 2012*, edited by D. J. Stokes and J. L. Hutchison (Royal Microscopical Society, Oxford, 2012), Vol. 2.

[6] L. Allen, M. J. Padgett, and M. Babiker, Prog. Opt. **39**, 291 (1999).

[7] L. Allen, S. M. Barnett, and M. J. Padgett, *Optical Angular Momentum* (Institute of Physics Publishers, Bristol, 2003).

[8] D. L. Andrews, *Structured Light and its Applications: An Introduction to Phase-Structured Beams and Nanoscale Optical Forces* (Academic Press, Burlington, 2008).

[9] D. G. Grier, Nature (London) **424**, 810 (2003).

[10] S. Lloyd, M. Babiker, and J. Yuan, Phys. Rev. Lett. **108**, 074802 (2012).

[11] F. Araoka, T. Verbiest, K. Clays, and A. Persoons, Phys. Rev. A **71**, 055401 (2005).

[12] M. Babiker, C. R. Bennett, D. Andrews, and L. Dávila Romero, Phys. Rev. Lett. **89**, 1 (2002).

[13] K. Y. Bliokh, M. R. Dennis, and F. Nori, Phys. Rev. Lett. **107**, 174802 (2011).

[14] J. Verbeeck, P. Schattschneider, S. Lazar, M. Stoger-Pollach, S. Loffler, A. Steiger-Thirsfeld, and G. Van Tendeloo, Appl. Phys. Lett. **99**, 203109 (2011).

[15] D. Newbury, *Principles of Analytical Electron Microscopy*, edited by J. Goldstein, D. Joy, and A. Romig (Springer, New York, 1986).

[16] A. I. M. Rae, *Quantum Mechanics* (Institute of Physics Pub., Bristol, 2002), 4th ed.

[17] F. Gross, *Relativistic Quantum Mechanics and Field Theory* (Wiley-Interscience, New York, 1999).

[18] S. Gasiorowicz, *Quantum Physics* (Wiley, New York, 2003), 3rd ed.